

Article

Adsorption of Oil by 3-(Triethoxysilyl) Propyl Isocyanate-Modified Cellulose Nanocrystals

Mehdi Jonoobi ^{1,2,*}  and Tizazu H. Mekonnen ^{2,*}

¹ Department of Wood and Paper Science and Technology, Faculty of Natural Resources, University of Tehran, Karaj 31587-77871, Iran

² Department of Chemical Engineering, University of Waterloo, Waterloo, ON N2L 3G1, Canada

* Correspondence: authors: mehdi.jonoobi@ut.ac.ir (M.J.); tmekonnen@uwaterloo.ca (T.H.M.)

Abstract: Oil leaks into water bodies and increased organic pollutants harm the environment and ecosystem in several ways, and cleaning up oil spills from water bodies is a global challenge. This research aimed to construct modified cellulose nanocrystal (CNC) based aerogels with 3-triethoxysilyl propyl isocyanate (TEPIC) to evaluate their potential application in oil adsorption. Here, a freeze-drying method was employed to make CNC aerogels. The aerogels were characterized using scanning electron microscopy (SEM), Brunauer–Emmett–Teller (BET) analysis, porosity and density measurements, Fourier transform infrared spectroscopy (FTIR), water contact angle (WCA) measurement, compressive strength, and oil adsorption capacity. SEM results confirmed that the aerogels have a largely porous structure, including a community of uniformly interconnected cellulose fibers. Moreover, the studied aerogels had a low density due to the high porosity. Also, the small pore diameter and high specific surface area were confirmed by the BET evaluation. FTIR confirmed the existence of functional groups and strong hydrogen bonding between CNC/TEPCI/Urea molecules. All TEPIC-modified CNC aerogels had water contact angle values greater than 130° indicating their hydrophobicity. The highest oil and glycerol adsorption was obtained with the use of modified CNC aerogels. Thus, the sample modified with 3 wt% TEPIC showed the highest adsorption capacities of 130 ± 7.22 , 120 ± 4.75 , and 95.28 ± 4.82 gg^{-1} for motor oil, vegetable oil and glycerol, respectively. The results of this study showed that ultra-light, hydrophobic and oil adsorbent materials based on chemically modified CNC aerogels can successfully be fabricated.

Keywords: cellulose nanocrystals; triethoxysilyl propyl isocyanate; aerogel; oil adsorption



Citation: Jonoobi, M.; Mekonnen, T.H. Adsorption of Oil by 3-(Triethoxysilyl) Propyl Isocyanate-Modified Cellulose Nanocrystals. *Processes* **2022**, *10*, 2154. <https://doi.org/10.3390/pr10102154>

Academic Editor: Selestina Gorgieva

Received: 11 September 2022

Accepted: 19 October 2022

Published: 21 October 2022

Publisher's Note: MDPI stays neutral with regard to jurisdictional claims in published maps and institutional affiliations.



Copyright: © 2022 by the authors. Licensee MDPI, Basel, Switzerland. This article is an open access article distributed under the terms and conditions of the Creative Commons Attribution (CC BY) license (<https://creativecommons.org/licenses/by/4.0/>).

1. Introduction

Given the frequency of oil spills and rising flow of greasy domestic and industrial wastewater, cleaning up oil spills from water bodies is a global challenge [1]. These concerns have led many researchers from different disciplines to collaborate to address the issue. Several solutions have been put forward to mitigate the oil leaks challenge that can be categorized into chemical, biological, and physical strategies. Chemical processes like in-situ burning, dispersion, and solidification are inexpensive and straightforward. The employment of microorganisms for degrading oily hydrocarbons via biological processes can also be useful but time-consuming. Their activity is usually influenced by various factors, including pH, temperature, oxygen levels, organic species, and others. Physical methods are also frequently used to contain the oil spill, but the effectiveness of skimmer and boom oil removal is constrained [2,3]. Physical absorption has garnered interest in containing oil spills in recent years because of its low energy consumption, low cost, simplicity of operation, and environmental safety [2–4]. The use of inorganic minerals, for instance, exfoliated graphite, vermiculite, flash, diatomaceous, etc. with low oil adsorption capacity is another physical strategy to mitigate oil spills.

On the other hand, despite having a high interaction with oil, synthetic organic adsorbents (such as polypropylene, polyurethane, etc.) degrade slowly, so the generated

waste causes environmental concern. Natural organic materials, such as sawdust, wool, kapok fiber, sugar cane bagasse, rice and coconut shells, chitosan, and cellulose [2,3,5–7], are appealing alternatives. In general, excellent hydrophobicity and lipophilicity, high load capacity, quick oil adsorption rate, low cost, and high buoyancy are necessary attributes for a highly effective oil adsorbent material [8,9]. Thus, synthetic superhydrophobic oil-adsorbing organic polymers are very attractive due to their high hydrophobicity, oil/water selectivity, and high efficacy in recovering oil from the surface [1,10]. However, the environmental impact of manufacturing these materials, their high costs in some cases as a result of the cost of raw materials and manufacturing process difficulty, and their frequent use on a large scale is limited [1]. Thus, there is a great demand for developing cost-effective, environmentally friendly, high oil adsorption sorbent materials for oil spill cleanup [3,11]. One of the most appropriate adsorbents in this regard is the use of aerogels due to their high specific surface area, good mechanical and structural integrity, easy operation, and high capacity to adsorb oil pollution from the water surface [12].

Aerogels are materials with high porosity, high surface area, greater flexibility, lightweight, and excellent processability and can withstand loads many times their own load [3,13]. A wide range of applications, including electrical conductors, supercapacitors, energy storage, gas sensors, detectors, catalyst support, heat and sound insulation, cell culture models, air filters, water filters, skin tissue engineering scaffolds, drug carriers, and adsorbents are possible for aerogels [3,6,14,15]. Cellulose nanocrystals (CNC) are perhaps the most widely used precursors for aerogels compared with those made from petrochemical sources [16–18]. High aspect ratio, high specific surface area, high crystallinity index, biodegradability and environmental friendliness, high specific mechanical strength, safety, low density, availability of different biological resources/waste, and ease of modification due to the abundance of hydroxyl groups (OH) are some of the appealing and distinctive characteristics of CNC for their use in functional aerogels [19,20]. The low density, excellent flexibility, high porosity, and strong adsorbence of CNC aerogel have been drawing interest [3]. These unique and promising advantages facilitate the use of CNC and eliminate the safety problems associated with synthetic polymers. Despite the appealing properties of CNC aerogels, they also have limitations that make their use difficult. Their main limitations are their inherent hydrophilicity that emanates from the OH in the molecular structure of cellulose [21], which causes them to not disperse well in many solvents and polymers causing the aggregation of the nanofibers. This inherent hydrophilicity of the CNC nanofibers is an important limiting factor for the adsorption of oil from water surface, which needs to be resolved via chemical modification of the CNCs' surface [22]. Therefore, the chemical modification of CNCs' surfaces by using appropriate functional groups to boost their reactivity with the substrate is usually employed. Depending on the translational use, chemical modification of the CNC can be performed at the OH of the glucose units on the crystal framework [16,23].

In general, the leakage and discharge of petroleum-contaminated wastewater are important environmental concerns. They not only lead to widespread pollution of the oceans and ecological system but also have adverse effects on the economy and tourism activities. In addition to oil pollutants, industrial oil effluents are other important environmental concerns, so if industrial oil effluents are not properly treated, they can cause risks to the ecosystem and human health [24,25]. For these reasons, there is extensive research interest in separating pollution from water and air [26]. Thus, the objective of this work was to fabricate functional CNC aerogels and evaluate their oil adsorption performance with a target of oil spill cleanup applications. The impact of incorporating urea as a CNC dispersing agent and citric acid as a crosslinking agent on the physico-chemical and oil adsorption of the aerogel was investigated. Additionally, the oil adsorption performance of the aerogel as a result of CNC modification with a silylating agent, triethoxysilyl propyl isocyanate (TEPIC), was studied. A simple freeze-drying followed by a low-temperature crosslinking process was employed to fabricate the CNC aerogels.

2. Materials and Methods

2.1. Materials

Cellulose nanocrystal (CNC) with a degree of polymerization of 175 was purchased from Weidmann Company (Zürich, Switzerland). To modify the CNC aerogel, 3-(triethoxysilyl) propyl isocyanate ($C_{10}H_{21}NO_4Si$) (TEPIC) 99% with $M_w = 247.37 \text{ gmol}^{-1}$ was provided by Merck Co. (Darmstadt, Germany). Urea ($CO(NH_2)_2$) 99.5% with $M_w = 60.056 \text{ gmol}^{-1}$ was purchased from Sigma Aldrich (St. Louis, MI, USA). The Citric acid ($C_6H_8O_7$) (CA) used as a crosslinker was purchased as a powder from Sigma Aldrich (St. Louis, MI, USA). Vegetable (corn) oil with viscosity $33.9 \text{ mm}^2/\text{s}$ and density 0.918 g/mL was obtained from a local grocery store (Waterloo, ON, Canada). Motor oil with a viscosity and density of $31.2 \text{ mm}^2/\text{s}$ and 0.892 g/mL , respectively, was obtained from an automotive parts store (Waterloo, ON, Canada). Glycerol with a viscosity of $37.4 \text{ mm}^2/\text{s}$ and density of 1.412 g/mL was purchased from Sigma Aldrich Canada (Oakville, ON, Canada). All solutions were prepared using deionized water.

2.2. Aerogel Preparation

CNC (2 wt.%) was mixed with deionized water. Next, The TEPIC was added to the CNC suspension at concentrations of 3 and 6 wt% (with respect to CNC) under vigorous stirring at room temperature for 3 h for the surface modification of CNC. Then, 3 wt% of CA crosslinking agent based on the CNC dry weight was added to the CNC/TEPIC suspension. The CNC/TEPIC/CA mixtures were stirred at room temperature for 6 h. In the next step, 50 wt% urea powder based on the CNC dry weight was added. The mixture (CNC/TEPIC/CA/Urea) was stirred at room temperature for 24 h (Table 1).

Table 1. The CNC, TEPIC, CA, and Urea content percentage for each treatment group.

	CNC Concentration (wt%)	TEPIC Concentration (wt%)	CA Concentration (wt%)	Urea Concentration (wt%)
C ₁	2	-	-	-
C ₂	2	-	3	-
C ₃	2	-	-	50
C ₄	2	-	3	50
C ₅	2	3	-	-
C ₆	2	6	-	50
C ₇	2	3	-	50
C ₈	2	3	3	50

To prepare the aerogels, the bottom 4 cm of a copper cylinder (4 cm diameter and 10 cm length) was placed in liquid nitrogen at a temperature of $-196 \text{ }^\circ\text{C}$, and a 3 cm diameter Teflon tube was fixed on the transverse surface. Then, the prepared mixtures with a volume of 20 mL were poured into a polytetrafluoroethylene (PTFE) (Teflon) tube. Next, the mixtures were slowly frozen from bottom to top. The frozen samples were lyophilized (CHRIST ALPHA 1-2 LD, (Osterode am Harz, Germany) at a condenser temperature of $-57 \text{ }^\circ\text{C}$, under a vacuum of 2.2 mbar for 48 h to produce a completely dry aerogel (Figure 1 schematic). Finally, the samples were placed in an oven at $40 \text{ }^\circ\text{C}$ for 24 h to evaporate the extra water because CA has to lose water to make cross-links. To create the cross-links, they were then placed in an oven set at $80 \text{ }^\circ\text{C}$ for 8 h. To finish the cross-linking process, the produced aerogel was placed in a vacuum oven at $50 \text{ }^\circ\text{C}$ for 24 h. Figure 2 shows the digital photographs of the final manufactured samples.

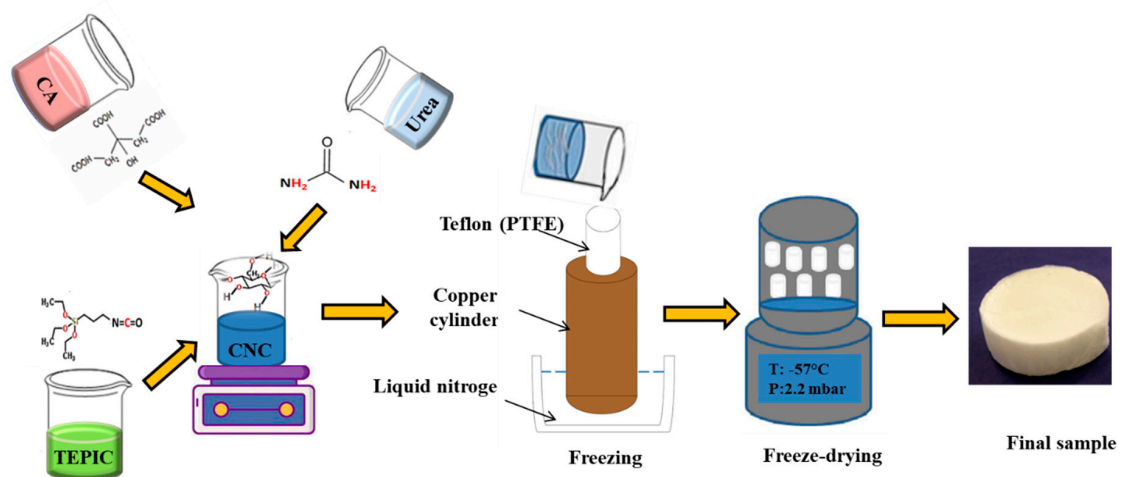


Figure 1. Schematic of the fabrication method of the CNC aerogels.

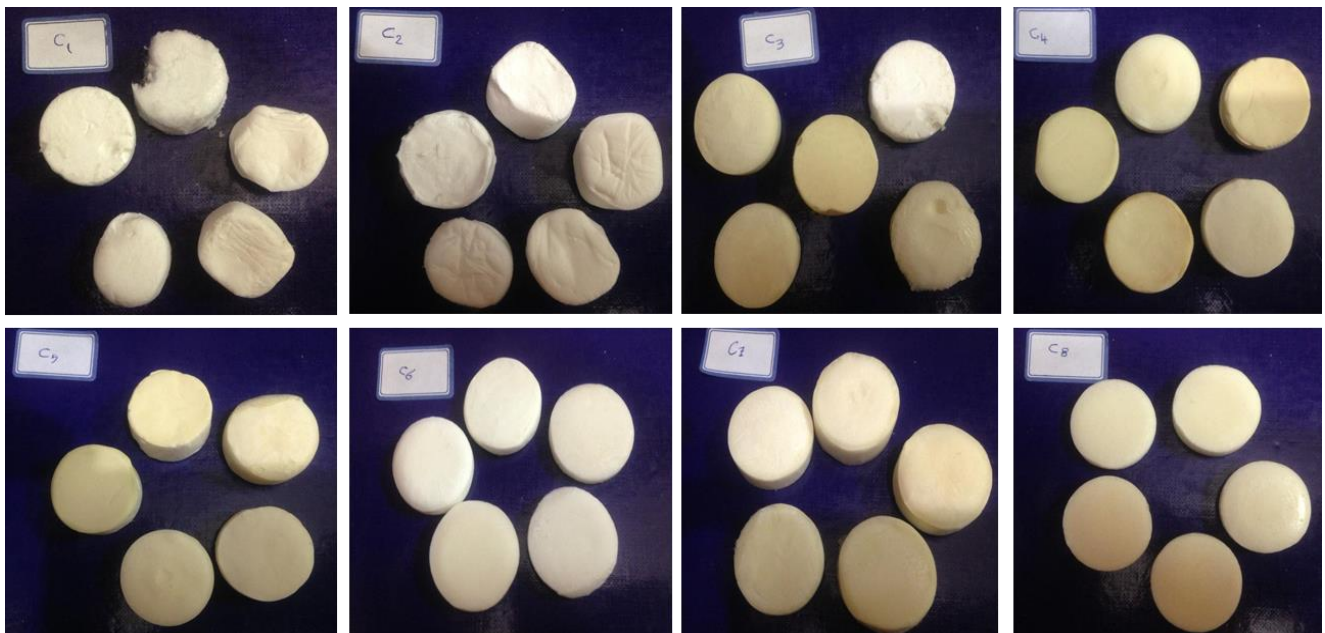


Figure 2. Digital photographs of samples freeze-dried.

2.3. Characterizations

2.3.1. Scanning Electron Microscopy (SEM)

Scanning electron microscopy (SEM) (JXA 840, JEOL Company, Akishima, Tokyo, Japan) was used to observe the cross-sectional images of the prepared aerogels at a voltage of 20 kV. The prepared samples were attached to copper stubs with mutual conductive adhesive tape and coated with a gold layer about 15 nm thick using a sputter coater.

2.3.2. Density and Porosity

The bulk density of the manufactured sample was calculated by measuring the mass and volume of each cylindrical CNC aerogel. The weight of the aerogel was determined by an analytical balance (0.1 mg accuracy, Mettler Toledo, Columbus, OH, USA), and the size of the aerogel (diameter and height) was determined using a digital caliper (0.01 mm

accuracy). The aerogel porosity was calculated using Equation (1), where ρ_a is the aerogel density and ρ_c ($\rho_c = 1.50 \text{ g/cm}^3$) is the density of CNC.

$$\text{Porosity (\%)} = \left(1 - \frac{\rho_a}{\rho_c}\right) \times 100 \quad (1)$$

2.3.3. Brunauer–Emmett–Teller (BET) Analysis

The specific surface areas of the prepared aerogels' were determined using Brunauer–Emmett–Teller (BET) using TriStar II Micromeritics and physical N_2 adsorption (Instrument Corp., Hauppauge, USA). Aerogel samples (0.1–0.2 g) were dried for 4 h at $115 \text{ }^\circ\text{C}$ before degassing for 18 h at $115 \text{ }^\circ\text{C}$. This was followed by an N_2 adsorption analysis at $-196 \text{ }^\circ\text{C}$. BET analysis was performed at $-196 \text{ }^\circ\text{C}$ for a relative vapor pressure (P/P_0) of 0.01–0.3. The mean pore size of the CNC aerogels has not changed, according to the Barrett–Joyner–Halender analysis, and is estimated from the nitrogen desorption isotherm (BJH).

2.3.4. Fourier Transform Infrared Spectroscopy (FTIR)

The change in the functional groups of unmodified CNC and modified CNC aerogels were examined using Fourier transform infrared spectroscopy (FTIR) with FTIR (Nicolet FTIR 6700, ThermoFisher Scientific, Massachusetts, USA) in the range of $400\text{--}4000 \text{ cm}^{-1}$ in KBr pellets with a resolution of 4 cm^{-1} .

2.3.5. Water Contact Angle (WCA)

To investigate the water repellency of CNC aerogels, the water contact angle (WCA) was measured using a G10 unit (Kruss Company, Hamburg, Germany). Using a sessile drop, water droplets with a volume of about $5 \text{ }\mu\text{L}$ were dispensed onto the surface of the aerogels. WCA values were calculated using Droplet Shape Analysis software (DSA100). Different measurements were taken on the CNC aerogel surface at various locations, and the average values obtained from multiple measurements were reported.

2.3.6. Compression Testing

Compression testing was carried out on an AGSX Shimadzu (Kyoto, Japan) according to ASTM D882 equipped with a 50 N load cell and STM-Controller software. At a crosshead speed of 1 mm min^{-1} , the stress-strain curves of the unmodified and modified CNC aerogels with a cylindrical shape (diameter = 28 mm; height = 12 mm) and with $n = 3$ samples were determined.

2.3.7. Oil Adsorption

Next, we determined how well unmodified and modified CNC aerogel adsorbed vegetable oil, motor oils, and glycerol. To ensure swelling equilibrium before the test, cylindrical aerogels with 28 mm diameters and 12 mm heights were weighted (W_{initial}) and submerged in a beaker that contains 50 g oil (or glycerol) and a 50 g water layer for an hour at room temperature. In the water–glycerol system, the aerogel samples were dipped gently and within 1 min of preparing the system to avoid solubilizing the glycerol in the water phase. After impregnation, the aerogels were carefully lifted from the container using a stainless-steel mesh basket. Any extra oil was allowed to be released for a minute before wiping the samples' surface with paper towel. The adsorptive capacity (Q , gg^{-1}), which is the weight of substances adsorbed per unit weight of the original aerogel, and the weight of the samples after testing (W_{final}) were calculated using Equation (2):

$$Q = \frac{W_{\text{final}} - W_{\text{initial}}}{W_{\text{initial}}} \quad (2)$$

2.4. Statistical Analysis

The outcomes were examined using the statistical package SPSS in a fully randomized design with $n = 3$ samples (version 20.0). All data are presented as mean \pm standard deviation and data comparison was conducted with (ANOVA) and then Duncan's Multi-Range test at a 95% confidence level.

3. Results and Discussion

3.1. SEM

SEM was employed to examine the morphology of unmodified and modified CNC aerogels, and the results are shown in Figure 3. All the aerogels have a highly porous structure made up of an interconnected web of uniform cellulose fibers indicating that the CNC was successfully self-assembled via hydrogen bonding to form a 3D porous network [3]. As noted in Figure 3, the unmodified CNC-based aerogels (C_1 , C_2 , C_3 , and C_4) have a porous matrix with relatively good dispersion. With the modification of the CNC with TEPIC (C_5 , C_6 , C_7 , and C_8), the aerogels' structure appears to be less porous (Figure 3). The tighter morphology of the modified specimen can be ascribed to the replacement of the CNC's -OH groups with TEPIC, which inhibits disruption by the urea [16]. Aerogel samples, including C_1 , C_4 , C_6 , and C_7 , displayed sheet-like morphology. However, C_6 , which contains a higher concentration of TEPIC (6 wt.%), generated a pronounced sheet-like structure that appeared to reduce the pore diameter.

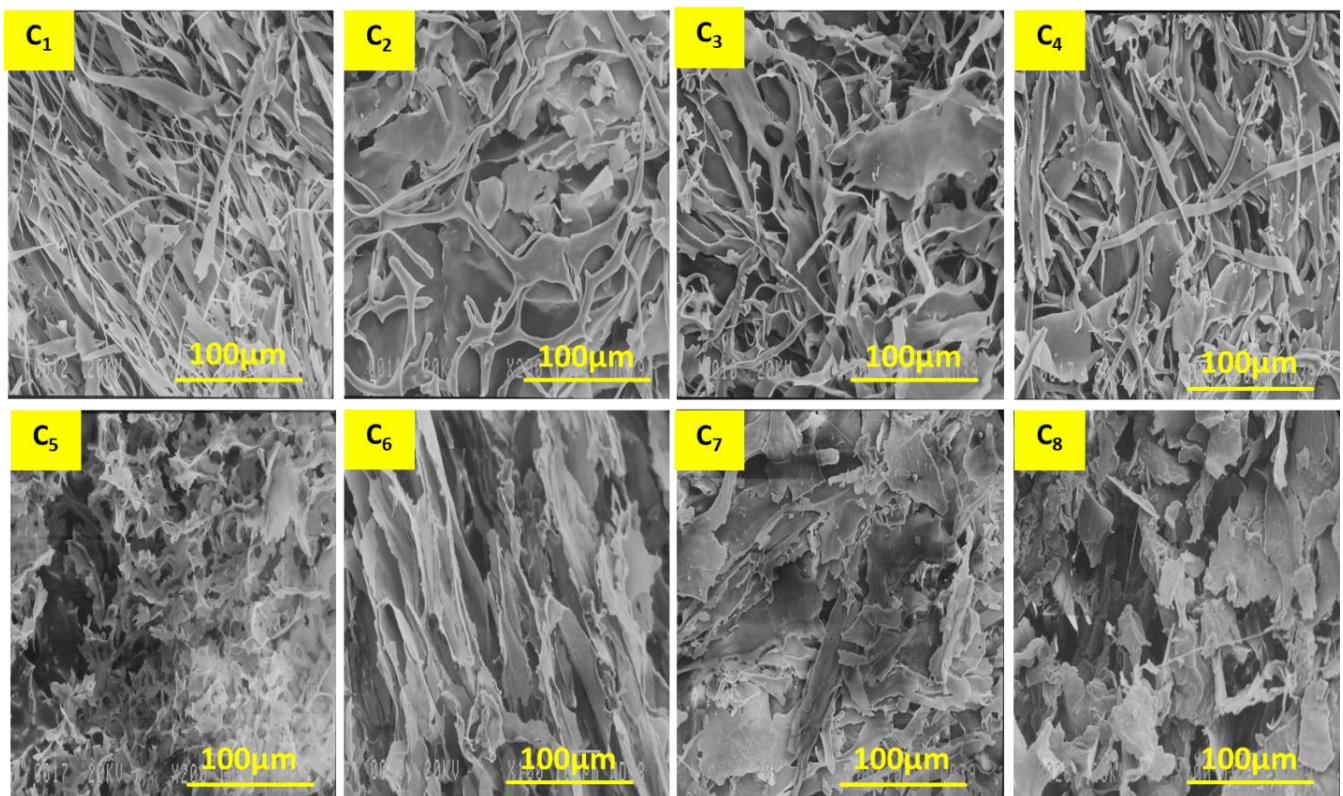


Figure 3. SEM images of the unmodified CNC and modified CNC aerogels with different concentrations of TEPIC/CA/Urea.

3.2. Aerogel Characteristics

The densities, porosities, specific surface areas, and pore sizes for unmodified and TEPIC-modified CNC aerogels are shown in Table 2. At a 95% confidence level, the analysis of variance results demonstrated a significant impact of the surface modification on the density, specific surface area, porosity, and pore size of the resulting aerogels. A Duncan

multiple-range test revealed that the difference in mean density in aerogels made using CNC without any modifications statistically significant. The aforementioned properties, however, differ significantly with surface modification. Upon the surface modification of CNC with TEPIC, the structure of C₄, C₅, C₆, and C₇ aerogels becomes denser and more compact, which results in an increase in density [2,3,27]. While urea appears to prevent CNCs aggregation, its impact seems limited for the modified CNCs [16]. This is because the TEPIC modification that provides the CNC with hydrophobic characteristics limits its interaction with the polar urea, and as a result, the CNC will be mostly aggregated [16,28,29]. As a result, the modified CNC-based aerogels are denser with reduced pore size. In other words, the size of the pore and volume of pores decreased due to its high density, which makes the aerogels compressed and denser [14,27,30,31].

Table 2. BET surface area, size of pores and volume of pores CNC and TEPIC-CNC aerogels.

Sample	Density (mg/cm ³)	BET (m ² /g)	Aver. Size of Pores (nm)	Porosity (%)	Volume of Pores (cm ³ /g)
C ₁	8.5 ± 0.54 ^e	214 ± 16.8 ^e	29.2 ± 1.81 ^a	99.3 ± 0.82 ^a	95.2 ± 3.18 ^a
C ₂	8.9 ± 0.46 ^{de}	227 ± 14.2 ^e	28.9 ± 1.21 ^a	99.2 ± 1.01 ^a	93.6 ± 4.32 ^a
C ₃	9.4 ± 0.36 ^d	231 ± 8.2 ^{de}	28.7 ± 1.43 ^{ab}	98.8 ± 0.92 ^{ab}	85.6 ± 3.22 ^b
C ₄	10.1 ± 0.76 ^{cd}	244 ± 18.2 ^d	27.4 ± 1.03 ^b	98.6 ± 0.32 ^{ab}	72.1 ± 4.32 ^c
C ₅	12.4 ± 0.82 ^b	262 ± 11.2 ^c	26.1 ± 1.02 ^b	98.3 ± 0.32 ^{ab}	69.7 ± 2.42 ^{cd}
C ₆	13.7 ± 0.56 ^b	298 ± 8.8 ^{ab}	23.6 ± 1.08 ^c	98.2 ± 0.48 ^{ab}	66.4 ± 3.38 ^d
C ₇	15.6 ± 0.87 ^a	311 ± 8.8 ^a	21.8 ± 1.16 ^d	97.9 ± 0.16 ^b	63.5 ± 3.62 ^{de}
C ₈	16.4 ± 0.71 ^a	318 ± 10.7 ^a	18.7 ± 1.27 ^e	97.5 ± 0.47 ^b	58.2 ± 3.77 ^e

Different lowercase letters in the same column show the significant difference ($p < 0.05$).

3.3. Fourier Transform Infrared Spectroscopy (FTIR)

To evaluate the change in the functional groups of CNC as a result of the TEPIC-modification, the CNC aerogel and its modified counterpart are evaluated by collecting FTIR spectra, and the results are shown in Figure 4. The change in the peak size associated with the stretching vibration of the OH groups (3175 to 3488 cm⁻¹) is shown in Figure 4. The TEPIC-modified aerogels displayed reduced -OH peaks, which could be attributed to the interactions between CNC and TEPIC chains. The IR spectra of unmodified and modified CNC and the bands attributed to the C-H group vibrations were visible between 3000 and 2900 cm⁻¹. The bending mode of the OH groups that adsorbed moisture was attributed to the band at 1640 cm⁻¹ [3,32]. The spectra of C₃, C₄, C₆, C₇, and C₈ displayed a small new peak at a wavelength of about 1540 cm⁻¹, which was attributed to NH₂ wagging in the urea. The bands at 1432 and 1358 cm⁻¹ were caused by the bending of CH₂ and C-H, while the band at 1197 cm⁻¹ was caused by the stretching of C-O groups from the skeleton of the pyranose ring, and the band at 900 cm⁻¹ was attributed to the ring's stretching vibration. Following chemical modification of CNC with TEPIC, silane-related peaks between 815 and 800 cm⁻¹ (m(Si-C)), attributed to the stretching vibration of the Si-O-Si or Si-O-C or the bonds [3,32–34], and at 1279 cm⁻¹, which were likely related to the bending of the C-H bonding of the -CH₃ groups were noted in the modified specimen.

3.4. Water Contact Angle (WCA)

The water contact angle (WCA) was measured to determine how the surface modification affected the hydrophilicity/hydrophobicity of the CNC aerogel. The unaltered CNC aerogels quickly adsorbed the water droplets due to their numerous pore structures and inherent hydrophilicity (Figure 5 (C_{1,2,3,4})), and they lacked a detectable contact angle. In contrast, TEPIC-modified CNC aerogels (Figure 5 (C_{5,6,7,8})) with high WCA of 136° to 146° retained the water drops on their surface, proving their hydrophobicity. The hydrophobicity of the modified CNC aerogels is attributed to the hydrophobicity of the aliphatic silane-based modifying agent (TEPIC) [3,35].

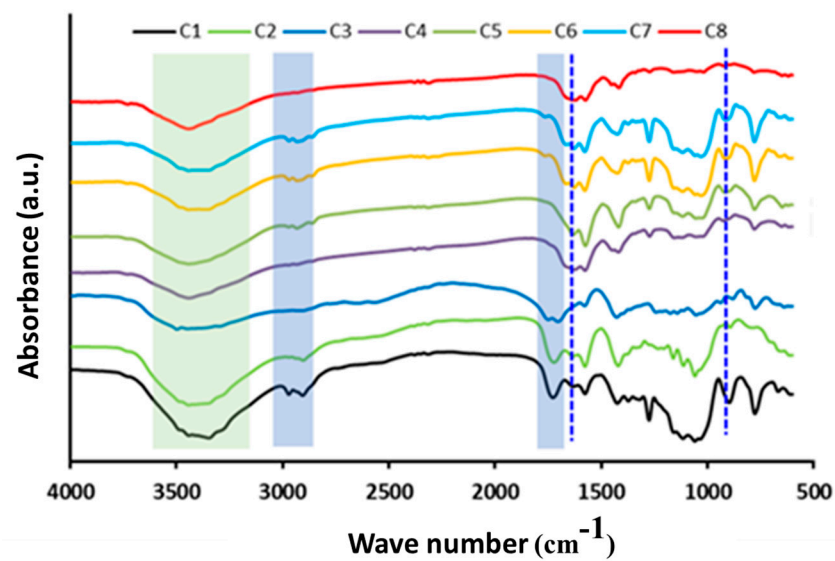


Figure 4. FTIR spectra of the unmodified CNC and modified CNC aerogels with different concentrations of TEPIC/CA/Urea. The dashed line indicates the change in peak trend and the appearance of new peaks.

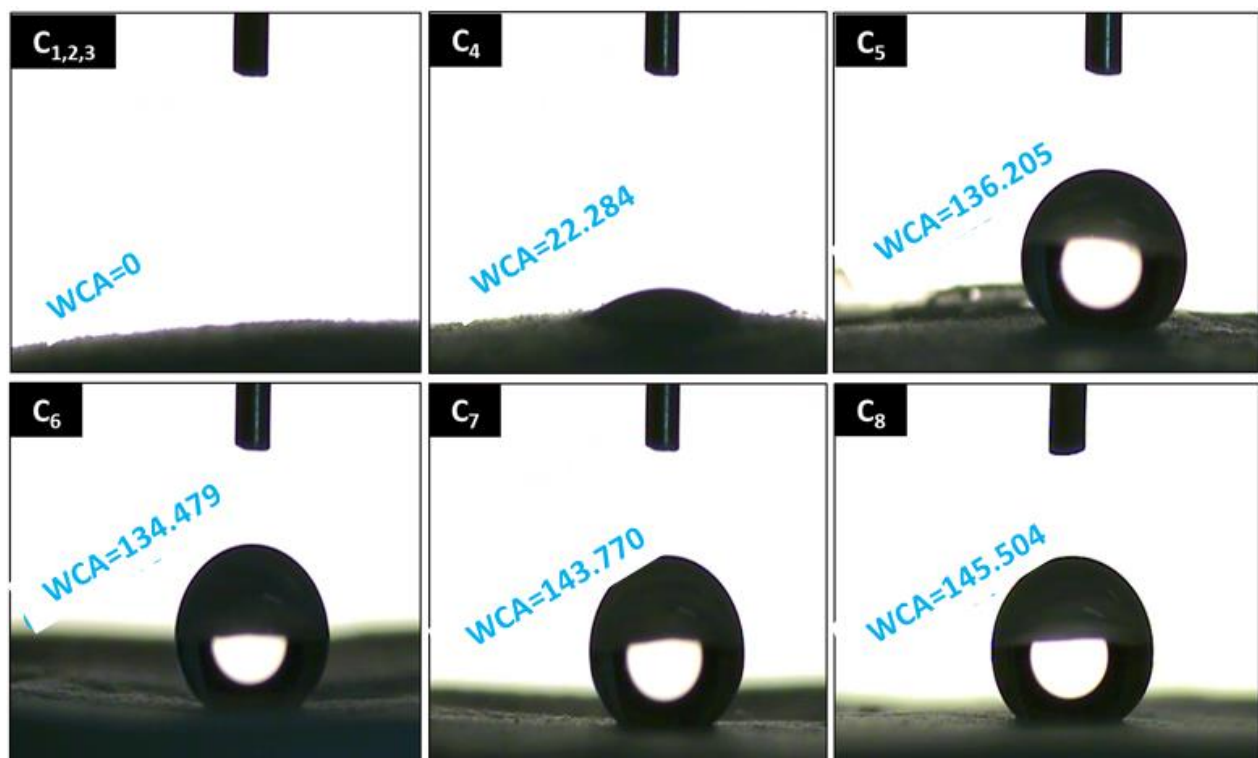


Figure 5. WCA of the unmodified and modified CNC aerogels.

3.5. Compression Testing

The compressive strength of the unmodified and TEPIC-modified CNC aerogels with various degrees of modifications was examined. The aerogels' compressive stress-strain curves are shown in Figure 6. The compressive stress-strain curves of all aerogels showed three stages: a linear elastic region, a non-linear plastic deformation plateau, and then dramatic stress increase at low, medium, and high strain, respectively [2,3,15]. The stress-strain relationship was linear at low strain, and the slopes got steeper as the density went up due to the applied compressive force. The primary deformation appears to be brought on by

prominent cellular pores collapsing or bending in elastic cell walls. Aerogel deformation at high strain could be a result of mesopore bending or damage, which breaks or compresses covalent bonds and causes the pore walls to start touching one another, forming the load-bearing parts [26,36,37]. At low strain (<25%), all aerogels composed of TEPIC-modified CNC appeared to have higher modulus. The presence of citric acid as a crosslinking agent seems to enhance the compressive strength of the unmodified CNC-based aerogels (C₂ and C₄) at a high strain rate (>25%). On the contrary, aerogels based on modified CNCs (C₇ and C₆) do not contain CA displayed higher modulus at high strain rates. C₈ aerogel, based on TEPIC-modified CNC, but also containing CA crosslinking agent, did not exhibit higher stress at low or high strain rates. This might be attributed to the interference of the TEPIC modification of CNC with the crosslinking reaction with citric acid.

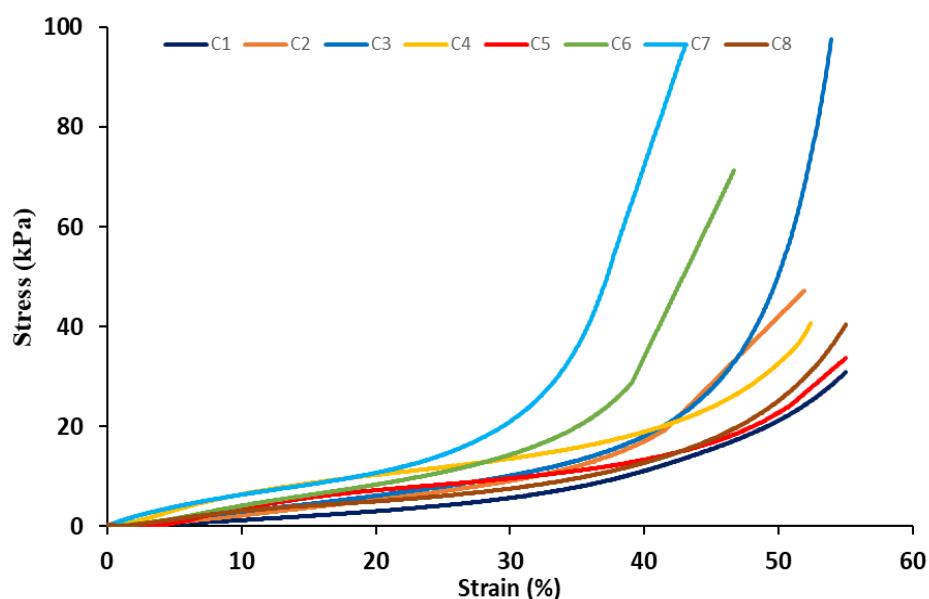


Figure 6. Compressive stress-strain curves of the unmodified and modified CNC aerogels.

3.6. Oil and Glycerol Adsorption

Due to the severe environmental damage and energy waste that oil spill accidents cause, oil removal from water has attracted significant academic and commercial interest [38,39]. In this study, the potential of low-density, sponge-like CNC aerogels as a potential candidate for removing organic pollutants from water because of their superhydrophobic and oleophilic qualities are evaluated. Because the sorption processes that take place are influenced by the chemical structures, micro- and macroporous structures of sorbent fibrous materials, as well as the inter- and intra-fiber interactions of the materials [40], the effect of CNC aerogel modification on the oil adsorption was evaluated. Because chemical interactions, such as intramolecular and van der Waals interactions, are the primary causes of the oil adsorption to the aerogel's surface, evaluating the effect of CNC surface modification on oil adsorption is important [40]. Additionally, the pore morphology and presence of capillary forces on aerogels are important factors for oil adsorption via [3,40].

Furthermore, the sorption process and prevention of oil leakage are greatly aided by surface roughness [4,41]. It was noted that the aerogels readily adsorb to cooking and glycerol.

The results of vegetable oil, motor oil, and glycerol adsorption on unmodified and TEPIC-modified CNC aerogel in 300 s and 1 h are shown in Table 3. Notably, the unmodified aerogel adsorbs oil at a slower rate than CNC that has undergone TEPIC modification. However, oil adsorption increased when urea was added to unaltered aerogels (C₃ and C₄). As expected, the TEPIC-modified CNC aerogels (C₅, C₆, C₇, and C₈) adsorb more oil

than unmodified CNC aerogels, which was due to the presence of the non-polar TEPIC chains on the aerogels' surface, as well as by their large specific surface area [3]. On the contrary, it was found that glycerol adsorption in all CNC aerogels was substantially lower than that of vegetable and motor oil. This might be attributed to glycerol's higher viscosity compared with vegetable and motor oils [3] in conjunction with its higher polarity. The amount of oil adsorption generally increased with increasing adsorption time.

Table 3. Oil adsorption of the unmodified and modified CNC aerogels.

Samples	After 300 s			After 1 h		
	Vegetable Oil (g g ⁻¹)	Motor Oil (g g ⁻¹)	Glycerol (g g ⁻¹)	Vegetable Oil (g g ⁻¹)	Motor Oil (g g ⁻¹)	Glycerol (g g ⁻¹)
C ₁	21.36 ± 3.38 ^d	25.24 ± 3.32 ^f	18.58 ± 1.18 ^e	29.37 ± 2.13 ^f	31.03 ± 2.18 ^f	26.09 ± 1.86 ^e
C ₂	12.23 ± 1.23 ^e	9.25 ± 0.42 ^g	9.89 ± 0.23 ^f	14.43 ± 1.02 ^g	12.10 ± 1.01 ^g	11.67 ± 0.92 ^f
C ₃	49.82 ± 3.23 ^c	48.67 ± 3.23 ^e	37.14 ± 2.31 ^d	58.43 ± 3.54 ^e	54.32 ± 3.57 ^e	41.90 ± 2.65 ^d
C ₄	51.80 ± 4.23 ^c	68.97 ± 3.43 ^c	43.25 ± 2.98 ^c	69.88 ± 4.12 ^d	83.67 ± 6.43 ^c	50.53 ± 3.82 ^c
C ₅	103.89 ± 7.32 ^a	109.65 ± 4.43 ^a	76.44 ± 4.39 ^b	120.51 ± 4.75 ^a	130.61 ± 7.22 ^a	95.28 ± 4.82 ^a
C ₆	102.53 ± 4.88 ^a	99.01 ± 3.43 ^b	76.14 ± 3.13 ^b	120.35 ± 5.28 ^a	122.95 ± 6.18 ^{ab}	87.51 ± 6.08 ^b
C ₇	88.21 ± 6.26 ^b	54.58 ± 4.54 ^d	38.79 ± 2.43 ^d	94.00 ± 3.16 ^c	77.03 ± 3.16 ^d	47.39 ± 3.26 ^c
C ₈	97.59 ± 5.17 ^{ab}	102.63 ± 2.32 ^b	86.21 ± 5.89 ^a	108.69 ± 7.03 ^b	115.69 ± 5.47 ^b	95.16 ± 4.67 ^a

Different lowercase letters in the same column show the significant difference ($p < 0.05$).

4. Conclusions and Future Perspectives

For the efficient separation of oil from water, a low-density material with high porosity and specific surface area was fabricated via the freeze-drying of CNC formulation dispersions. Oil leaks into water bodies and increased organic pollutants harm the environment and ecosystem in several ways. For the efficient separation of oil from water, a low-density material with high porosity and specific surface area was fabricated via the freeze-drying of CNC formulation dispersions. The high specific surface area and low density were advantageous for their application as an adsorbent. TEPIC deposition was used to transform the hydrophilic ultralight and porous aerogel into a hydrophobic material with a high-water contact angle. The aerogels quickly and reversibly adsorbed motor oil, vegetable oil, and glycerol after the modification. We observed that while incorporating urea improves the porosity of the aerogels, it significantly reduces the oil adsorption capacity due to the high polarity of urea. The improved performance of TEPIC-modified CNC aerogels in terms of greater oil adsorption capacity may be explained by the presence of non-polar and hydrophobic functional groups in TEPIC. The results of investigating the oil adsorption capacity of unmodified CNC aerogels showed that their oil adsorption rate is low due to the inherent hydrophilicity of CNC. However, the TEPIC-modified CNC aerogels' adsorption rate of motor oil increases compared with that of vegetable oil and glycerol in all aerogels. This increase was due to the low viscosity of motor oil compared with vegetable oil and glycerol, which allows the molecules of the low-viscosity motor oil to move faster through the pore channels than vegetable oil and high-viscosity glycerol, causing faster and greater adsorption [3,42,43]. Overall, the modified CNC aerogels can be appealing alternatives to commonly used oil spill cleaning adsorbents to remove oil spills from water bodies.

Author Contributions: Conceptualization, methodology, formal analysis, investigation, data curation, writing—original draft preparation, M.J.; writing—review and editing, M.J. and T.H.M.; supervision, project administration, M.J. and T.H.M.; resources, M.J. and T.H.M. All authors have read and agreed to the published version of the manuscript.

Funding: This research was funded by Natural Science and Engineering Research Council of Canada (NSERC) grant number RGPIN-2019-04112.

Institutional Review Board Statement: This study does not require moral approval, in other words, it is not applicable because it is not related to humans and animals study.

Informed Consent Statement: Not applicable.

Data Availability Statement: Data supporting reported results can be found provided up on reasonable request to the corresponding authors.

Acknowledgments: The authors are thankful to the University of Tehran, the University of Waterloo, Canadian Foundation for Innovation (CFI), and Natural Science and Engineering Research Council of Canada (NSERC) for the financial support of the project. Additionally, the authors would like to thank Sima Sepahvand for perform some laboratory tests.

Conflicts of Interest: The authors declare no conflict of interest.

References

1. Oribayo, O.; Feng, X.; Rempel, G.L.; Pan, Q. Synthesis of lignin-based polyurethane/graphene oxide foam and its application as an absorbent for oil spill clean-ups and recovery. *Chem. Eng. J.* **2017**, *323*, 191–202. [\[CrossRef\]](#)
2. Feng, J.; Nguyen, S.T.; Fan, Z.; Duong, H.M. Advanced fabrication and oil absorption properties of super-hydrophobic recycled cellulose aerogels. *Chem. Eng. J.* **2015**, *270*, 168–175. [\[CrossRef\]](#)
3. Rafeian, F.; Hosseini, M.; Jonoobi, M.; Yu, Q. Development of hydrophobic nanocellulose-based aerogel via chemical vapor deposition for oil separation for water treatment. *Cellulose* **2018**, *25*, 4695–4710. [\[CrossRef\]](#)
4. Zhu, K.; Shang, Y.Y.; Sun, P.Z.; Li, Z.; Li, X.M.; Wei, J.Q.; Wu, D.H.; Cao, A.Y.; Zhu, H.W. Oil spill cleanup from sea water by carbon nanotube sponges. *Front. Mater. Sci.* **2013**, *7*, 170–176. [\[CrossRef\]](#)
5. Lavoine, N.; Desloges, I.; Dufresne, A.; Bras, J. Microfibrillated cellulose—Its barrier properties and applications in cellulosic materials: A review. *Carbohydr. Polym.* **2012**, *90*, 735–764. [\[CrossRef\]](#)
6. Ghafari, R.; Jonoobi, M.; Amirabad, L.M.; Oksman, K.; Taheri, A.R. Fabrication and characterization of novel bilayer scaffold from nanocellulose based aerogel for skin tissue engineering applications. *Int. J. Biol. Macromol.* **2019**, *136*, 796–803. [\[CrossRef\]](#)
7. Yaqoob, A.A.; Parveen, T.; Umar, K.; Mohamad Ibrahim, M.N. Role of Nanomaterials in the Treatment of Wastewater: A Review. *Water* **2020**, *12*, 495. [\[CrossRef\]](#)
8. Wang, J.; Zheng, Y.; Wang, A. Coated kapok fiber for removal of spilled oil. *Mar. Pollut. Bull.* **2013**, *69*, 91–96. [\[CrossRef\]](#)
9. Umar, K.; Yaqoob, A.A.; Ibrahim, M.N.M.; Parveen, T.; Safian, M.T.U. Environmental applications of smart polymer composites. In *Smart Polymer Nanocomposite*; Woodhead Publishing: Sawston, UK, 2021; pp. 295–312. ISBN 9780128199619. [\[CrossRef\]](#)
10. Oribayo, O.; Feng, X.; Rempel, G.L.; Pan, Q. Modification of formaldehyde-melamine-sodium bisulfite copolymer foam and its application as effective sorbents for cleanup of oil spills. *Chem. Eng. Sci.* **2017**, *160*, 384–395. [\[CrossRef\]](#)
11. Nguyen, S.T.; Feng, J.; Ng, S.K.; Wong, J.P.; Tan, V.B.; Duong, H.M. Advanced thermal insulation and absorption properties of recycled cellulose aerogels. *Colloids Surf. A Physicochem. Eng.* **2014**, *445*, 128–134. [\[CrossRef\]](#)
12. Xu, Z.; Jiang, X.; Zhou, H.; Li, J. Preparation of magnetic hydrophobic polyvinyl alcohol (PVA)–cellulose nanofiber (CNF) aerogels as effective oil absorbents. *Cellulose* **2018**, *25*, 1217–1227. [\[CrossRef\]](#)
13. Baetens, R.; Jelle, B.P.; Gustavsen, A. Aerogel insulation for building applications: A state-of-the-art review. *Energy Build.* **2011**, *43*, 761–769. [\[CrossRef\]](#)
14. Sepahvand, S.; Jonoobi, M.; Ashori, A.; Gauvin, F.; Brouwers, H.J.H.; Oksman, K.; Yu, Q. A promising process to modify cellulose nanofibers for carbon dioxide (CO₂) adsorption. *Carbohydr. Polym.* **2020**, *230*, 115571. [\[CrossRef\]](#) [\[PubMed\]](#)
15. Sepahvand, S.; Jonoobi, M.; Ashori, A.; Rabie, D.; Gauvin, F.; Brouwers, H.J.H.; Yu, Q.; Mekonnen, T.H. Modified cellulose nanofibers aerogels as a novel air filters; synthesis and performance evaluation. *Int. J. Biol. Macromol.* **2022**, *203*, 601–609. [\[CrossRef\]](#)
16. Khanjanzadeh, H.; Behrooz, R.; Bahramifar, N.; Pinkl, S.; Gindl-Altmutter, W. Application of surface chemical functionalized cellulose nanocrystals to improve the performance of UF adhesives used in wood based composites-MDF type. *Carbohydr. Polym.* **2019**, *206*, 11–20. [\[CrossRef\]](#)
17. De France, K.J.; Hoare, T.; Cranston, E.D. Review of hydrogels and aerogels containing nanocellulose. *Chem. Mater.* **2017**, *29*, 4609–4631. [\[CrossRef\]](#)
18. Liang, L.; Zhang, S.; Goenaga, G.A.; Meng, X.; Zawodzinski, T.A.; Ragauskas, A.J. Chemically cross-linked cellulose nanocrystal aerogels for effective removal of cation dye. *Front. Chem.* **2020**, *8*, 570. [\[CrossRef\]](#)
19. Chaabouni, O.; Boufi, S. Cellulose nanofibrils/polyvinyl acetate nanocomposite adhesives with improved mechanical properties. *Carbohydr. Polym.* **2017**, *156*, 64–70. [\[CrossRef\]](#)
20. Jonoobi, M.; Ashori, A.; Siracusa, V. Characterization and properties of polyethersulfone/modified cellulose nanocrystals nanocomposite membranes. *Polym. Test.* **2019**, *76*, 333–339. [\[CrossRef\]](#)
21. Ebrahimi, A.; Dahrazma, B.; Adelifard, M. Facile and novel ambient pressure drying approach to synthesis and physical characterization of cellulose-based aerogels. *J. Porous Mater.* **2020**, *27*, 1219–1232. [\[CrossRef\]](#)
22. Zhou, X.; Fu, Q.; Liu, H.; Gu, H.; Guo, Z. Solvent-free nanoalumina loaded nanocellulose aerogel for efficient oil and organic solvent adsorption. *J. Colloid Interface Sci.* **2021**, *581*, 299–306. [\[CrossRef\]](#) [\[PubMed\]](#)
23. Lam, M.K.; Lee, K.T.; Mohamed, A.R. Current status and challenges on microalgae-based carbon capture. *Int. J. Greenh. Gas Control* **2012**, *10*, 456–469. [\[CrossRef\]](#)

24. Wahi, R.; Chuah, L.A.; Choong, T.S.Y.; Ngaini, Z.; Nourouzi, M.M. Oil removal from aqueous state by natural fibrous sorbent: An overview. *Sep. Purif. Technol.* **2013**, *113*, 51–63. [[CrossRef](#)]
25. Yang, W.J.; Yuen, A.C.Y.; Li, A.; Lin, B.; Chen, T.B.Y.; Yang, W.; Lu, H.D.; Yeoh, G.H. Recent progress in bio-based aerogel absorbents for oil/water separation. *Cellulose* **2019**, *26*, 6449–6476. [[CrossRef](#)]
26. Sepahvand, S.; Jonoobi, M.; Ashori, A.; Gauvin, F.; Brouwers, H.J.H.; Yu, Q. Surface modification of cellulose nanofiber aerogels using phthalimide. *Polym. Compos.* **2020**, *41*, 219–226. [[CrossRef](#)]
27. Sepahvand, S.; Bahmani, M.; Ashori, A.; Pirayesh, H.; Yu, Q.; Dafchahi, M.N. Preparation and characterization of air nanofilters based on cellulose nanofibers. *Int. J. Biol. Macromol.* **2021**, *182*, 1392–1398. [[CrossRef](#)] [[PubMed](#)]
28. Liu, H.; Wang, A.; Xu, X.; Wang, M.; Shang, S.; Liu, S.; Song, J. Porous aerogels prepared by crosslinking of cellulose with 1, 4-butanediol diglycidyl ether in NaOH/urea solution. *RSC Adv.* **2016**, *6*, 42854–42862. [[CrossRef](#)]
29. Long, L.Y.; Weng, Y.X.; Wang, Y.Z. Cellulose Aerogels: Synthesis, Applications, and Prospects. *Polymers* **2018**, *10*, 623. [[CrossRef](#)] [[PubMed](#)]
30. Rafieian, F.; Jonoobi, M.; Yu, Q. A novel nanocomposite membrane containing modified cellulose nanocrystals for copper ion removal and dye adsorption from water. *Cellulose* **2019**, *26*, 3359–3373. [[CrossRef](#)]
31. Rafieian, F.; Mousavi, M.; Yu, Q.; Jonoobi, M. Amine functionalization of microcrystalline cellulose assisted by (3-chloropropyl) triethoxysilane. *Int. J. Biol. Macromol.* **2019**, *130*, 280–287. [[CrossRef](#)] [[PubMed](#)]
32. Khanjanzadeh, H.; Behrooz, R.; Bahramifar, N.; Gindl-Altmutter, W.; Bacher, M.; Edler, M.; Griesser, T. Surface chemical functionalization of cellulose nanocrystals by 3-aminopropyltriethoxysilane. *Int. J. Biol. Macromol.* **2018**, *106*, 1288–1296. [[CrossRef](#)] [[PubMed](#)]
33. Zhang, Z.; Sèbe, G.; Rentsch, D.; Zimmermann, T.; Tingaut, P. Ultralightweight and flexible silylated nanocellulose sponges for the selective removal of oil from water. *Chem. Mater.* **2014**, *26*, 2659–2668. [[CrossRef](#)]
34. Özmen, N.; Sami Çetin, N.; Tingaut, P.; Sèbe, G. Transesterification reaction between acetylated wood and trialkoxysilane coupling agents. *J. Appl. Polym. Sci.* **2007**, *105*, 570–575. [[CrossRef](#)]
35. Shorey, R.; Gupta, A.; Mekonnen, T.H. Hydrophobic modification of lignin for rubber composites. *Ind. Crops Prod.* **2021**, *174*, 114189. [[CrossRef](#)]
36. Si, Y.; Yu, J.; Tang, X.; Ge, J.; Ding, B. Ultralight nanofibre-assembled cellular aerogels with superelasticity and multifunctionality. *Nat. Commun.* **2014**, *5*, 5802. [[CrossRef](#)] [[PubMed](#)]
37. Yang, X.; Cranston, E.D. Chemically cross-linked cellulose nanocrystal aerogels with shape recovery and superabsorbent properties. *Chem. Mater.* **2014**, *26*, 6016–6025. [[CrossRef](#)]
38. Xue, Z.; Cao, Y.; Liu, N.; Feng, L.; Jiang, L. Special wettable materials for oil/water separation. *J. Mater. Chem.* **2014**, *2*, 2445–2460. [[CrossRef](#)]
39. Yu, Y.; Wu, X.; Fang, J. Superhydrophobic and superoleophilic “sponge-like” aerogels for oil/water separation. *J. Mater. Sci.* **2015**, *50*, 5115–5124. [[CrossRef](#)]
40. Zanini, M.; Lavoratti, A.; Lazzari, L.K.; Galiotto, D.; Pagnocelli, M.; Baldasso, C.; Zattera, A.J. Producing aerogels from silanized cellulose nanofiber suspension. *Cellulose* **2017**, *24*, 769–779. [[CrossRef](#)]
41. Wu, Z.Y.; Li, C.; Liang, H.W.; Chen, J.F.; Yu, S.H. Ultralight, flexible, and fire-resistant carbon nanofiber aerogels from bacterial cellulose. *Angew. Chem.* **2013**, *125*, 2997–3001. [[CrossRef](#)]
42. Sayyad Amin, J.; Vared Abkenar, M.; Zendehboudi, S. Natural sorbent for oil spill cleanup from water surface: Environmental implication. *Ind. Eng. Chem. Res.* **2015**, *54*, 10615–10621. [[CrossRef](#)]
43. Ahuja, D.; Dhiman, S.; Rattan, G.; Monga, S.; Singhal, S.; Kaushik, A. Superhydrophobic modification of cellulose sponge fabricated from discarded jute bags for oil water separation. *J. Environ. Chem. Eng.* **2021**, *9*, 105063. [[CrossRef](#)]